

Microwave spectroscopy of Al I Rydberg states: F terms

S F Dyubko¹, V A Efremov¹, V G Gerasimov¹ and K B MacAdam²

¹ Department of Radiophysics, Kharkov National University, Svobody Square 4,
Kharkov 61077, Ukraine

² Department of Physics and Astronomy, University of Kentucky, Lexington,
KY 40506-0055, USA

E-mail: Victor.A.Efremov@univer.kharkov.ua and macadam@uky.edu

Received 17 June 2003, in final form 28 July 2003

Published 27 August 2003

Online at stacks.iop.org/JPhysB/36/3797

Abstract

Energy level separations in high-lying Rydberg states of neutral aluminium have been measured by a two-photon millimetre-wave resonance method to obtain $n^2F-(n+1)^2F$ intervals for $n = 29-37$ with an accuracy ± 1 MHz. An Al atomic beam was excited stepwise by pulsed lasers, and the Rydberg atoms were detected by state-selective field ionization. From these data and previous optical data for the $3s^2n\ell$ configuration of Al I new Ritz-expansion coefficients, which express the weakly n -dependent quantum defects for the nF Rydberg series, have been obtained. A previous laser-spectroscopic study of 2F Rydberg levels in Al I is shown to be in error, and quantum defects based on the classical spectroscopic work of Eriksson and Isberg are confirmed. The nF series is completely regular and shows no sign of perturbations by other electronic configurations.

1. Introduction

Rydberg states of neutral aluminium have not been definitively studied to date. Some laser and microwave resonance studies of Rydberg states in other atoms having outer-shell ground-state configurations s^2p (In, Ga and Tl) have been reported [1], but in Al, accuracies no better than ± 0.05 cm⁻¹ for states above $n = 10$ have been obtained. Accurate energies and splittings in high-lying states are important for trace element analysis [2] and for both optical and radio-astronomy [3]. In 1963, using photographic grating spectroscopy, Eriksson and Isberg [4] measured Al I emission lines connecting to 2S , 2P , 2D and 2F terms from $n = 4$ to 9 with an estimated accuracy ± 0.003 cm⁻¹. The energies of $3s^2nf^2F$ terms ($n = 4-8$) were calculated from these data to an accuracy ± 0.01 cm⁻¹ and the ionization limit was determined as $(48\,278.37 \pm 0.02)$ cm⁻¹. This ionization potential was confirmed by the same authors in 1967 [5] and refined in 1989 by Buurman *et al* [6] as $(48\,278.372 \pm 0.001)$ cm⁻¹.

On the basis of n^2F terms ($n = 4-8$) Eriksson and Isberg determined quantum defects and the Ritz coefficients that describe their weak n -dependence.

In 1984 Zherikhin *et al* [7] measured $3s^2nf^2F$ terms of Al I for $n = 11-55$ Rydberg states by two-step laser spectroscopy to an estimated accuracy $\pm 0.05 \text{ cm}^{-1}$. Their absolute wavelengths were determined by interpolation between suitable Ne hollow-cathode emission lines in a Fabry–Perot interferometer having free spectral range 1 cm^{-1} . From these data 2F quantum defects and the Al I ionization energy were found, whose accuracy, however, rests on that of the neon reference lines used and on the laser linewidth 0.2 cm^{-1} . The results were at variance with those of [4] and [5].

Determination of energy intervals between adjacent high-lying (Rydberg) states may be significantly improved if measurements are carried out at microwave frequencies [8]. Doppler broadening becomes insignificant and resonances become very narrow, limited instead by inverse observation time and by stray-field perturbations. On the other hand, such measurements require a more complicated experimental set-up. Microwave resonance methods have been extensively used to investigate Rydberg states of alkalis, alkaline earths, helium, molecular hydrogen and other systems [9]. The spectroscopy of aluminium in its normal Rydberg-state electronic configuration $1s^22s^22p^63s^2n\ell$ is not expected to be greatly dissimilar for $\ell \geq 3$ from that in alkalis (although it would have a substantially different core—primarily $3s^2$ —polarizability). In its nd Rydberg states, aluminium has unusually large spin–orbit fine-structure splittings [10] and has offered an important test case for multichannel quantum-defect theory [11].

As the first step in a high-precision investigation of Al Rydberg states $\ell = 0-4$, we have constructed a laser-microwave spectrometer for investigation of Rydberg states of Al I atoms and have measured frequencies of nine two-photon transitions of type $n^2F_{5/2,7/2} \rightarrow (n+1)^2F_{5/2,7/2}$ in the principal quantum number range $n = 29-37$ with accuracy of about 0.5 MHz, more than three orders of magnitude better than the optical measurements. We show moreover that the results of Zherikhin *et al* are apparently in error systematically by about 0.08 cm^{-1} (equivalent to about 2400 MHz) and we deduce that the 2F quantum defects and ionization energy determined earlier by Eriksson and Isberg and (in the case of the ionization energy) confirmed by Buurman *et al* are correct and reliable for use in both optical and microwave regimes. This establishes a necessary foundation for work of similar accuracy in S, P, D and G Rydberg states of Al I. To our knowledge this is the first investigation of Al Rydberg states by laser-microwave resonance spectroscopy.

2. Experimental details

A diagram of the apparatus is shown in figure 1. An incandescent tungsten (W) wire of diameter 0.5 mm and length 1.5 cm, covered with Al–Ni alloy, is used as an Al atomic-beam source in the spectrometer, prepared as follows. A 2 mg piece of Al is affixed by Ni wire of 0.1 mm diameter at the centre of the W heater and support wire. When heated to the melting point Al spreads over a 1 cm length of the Ni spiral. This results in formation of a drop of Al–Ni alloy of 1.0–1.5 mm diameter. When the drop is heated to 1000–1100 °C a uniform omnidirectional flow of Al atoms is obtained for 4–6 h. (This is similar to the methods described by Strong [12].) An atomic beam is formed from the thermally emitted vapour by a $2 \times 10 \text{ mm}$ aperture mounted 60 mm from the emitter just before entry of the beam between capacitor plates that are used for field ionization [9] of laser-excited Rydberg atoms.

Al atoms are pumped to Rydberg nF states by two-step pulsed laser excitation (see figure 2) between the plates: the upper level $3^2P_{3/2}$ of the doublet ground state is excited to $3^2D_{3/2,5/2}$ by ultraviolet light at $\lambda_1 = 309.27 \text{ nm}$. From $3D$, the Rydberg states $n^2F_{5/2,7/2}$ are reached by red

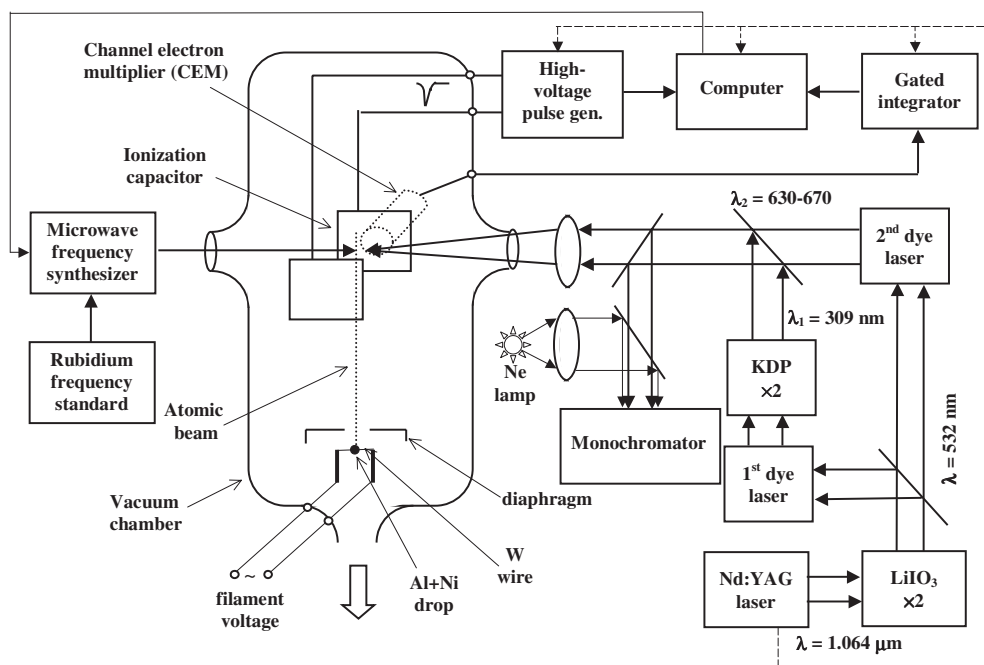


Figure 1. Apparatus layout. A collimated aluminium vapour beam in vacuum is excited to Rydberg states by merged light from two dye lasers. Atoms are field-ionized and detected in a CEM. An auxiliary monochromator, aided by a Ne spectrum lamp, is used for initial line-up and identification of Rydberg states. Microwaves are introduced via a horn antenna through a quartz window from outside the vacuum.

light at $\lambda_2 = 630\text{--}670$ nm. UV light for the first step was obtained by doubling the output of a rhodamine-B dye laser in a KDP nonlinear crystal. The second-step dye laser used oxazine-17 dye. The dye lasers were pumped together by the 532 nm second harmonic of a Q-switched Nd:YAG laser at 12.5 Hz repetition rate. The pulse energies of the first- and second-step lasers were 3–10 and 20–50 μJ , respectively. The laser linewidths were 0.5–1.0 cm^{-1} .

The two laser beams were merged using a dichroic mirror and were then directed between parallel-plate electrodes by a long-focus CaF lens. The electrodes had diameter 40 mm and spacing 6.5 mm. A zone of Al Rydberg excitation was formed at the centre of the plates opposite a pattern of input holes in front of a channel electron multiplier (CEM). The cloud of Rydberg atoms was cylindrical having 1–2 mm diameter and about 1 cm length. Microwave radiation of power level 10–1000 μW was introduced between the plates from an external horn antenna through a quartz window into the vacuum. A frequency synthesizer and crystal harmonic multiplier provided continuous millimetre-wave radiation at 50–120 GHz. The synthesizer was controlled by a small computer, which also provided data acquisition and processing functions. At the beginning of each measurement session the synthesizer's reference oscillator was calibrated by a Rb frequency standard. Detection of Rydberg atoms that had undergone a microwave transition was carried out by selective field ionization (SFI) [9]. High-voltage pulses for SFI were applied to the plates 0.2 μs after the laser pulse and the effective exposure time of Rydberg atoms to microwaves was limited to about 1 μs before the levels were abruptly Stark-shifted out of resonance by the leading edge of the SFI pulse.

Initial tuning of the two-step excitation lasers was aided by the close coincidence of the required 3P–3D wavelength $2\lambda_1 = 618.54$ with the 616.3 nm orange line from a neon standard

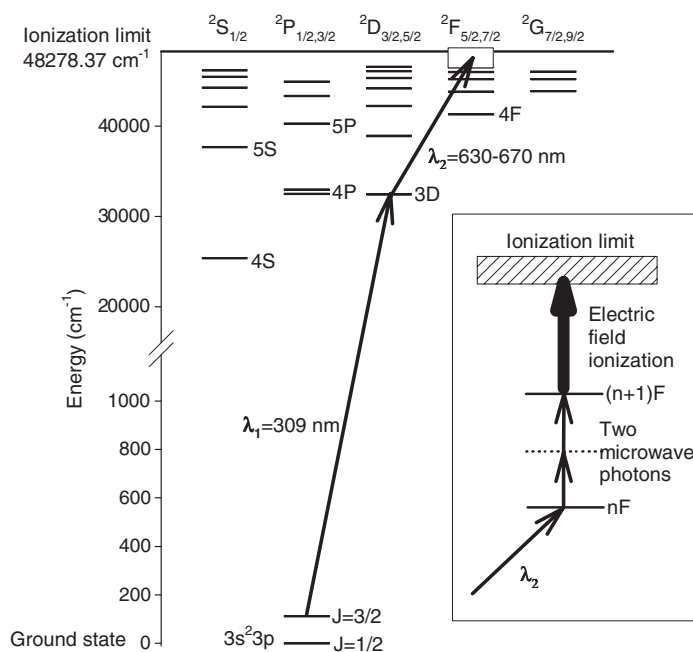


Figure 2. The Al I energy level and stepwise excitation scheme. Inset: two-photon microwave resonance via a virtual intermediate state (dotted), followed by pulsed field ionization for detection of the transition to the upper level. The F-state doublet fine structure is unresolved.

discharge lamp, observed in an auxiliary monochromator. By allowing residual fundamental laser light together with second-harmonic UV light at the output of the KDP crystal to reach the Al vapour beam, resonantly enhanced photoionization was readily observed to signal the correct laser tuning. A small constant voltage was applied across the plates at this point to sweep photoelectrons into the CEM. When a suitable short-pass filter was placed after the KDP crystal this resonance photoionization signal disappeared. Next the second-step laser was tuned close in wavelength to another suitable line of the neon standard lamp where it was capable of exciting an unresolved continuum of Al $3D \rightarrow nF$ transitions for $n > 50$ in the presence of a modest constant ionizing field applied to the ionization plates. Once this Rydberg-atom continuum signal was obtained, laser alignment and frequency tuning could be optimized under conditions of pulsed field ionization. Individual field-free states in the vicinity of $n = 30$ were resolved and their identifications were confirmed by wavelength measurements.

After the second-step (red) laser was tuned to the desired value of n the amplitude of the SFI pulse voltage was decreased until the CEM ion current was reduced significantly. When microwaves were tuned onto a two-photon $nF \rightarrow (n+1)F$ microwave resonance, the ion current following field ionization increased, corresponding to transition to the higher more weakly bound $(n+1)F$ state (figure 2). The analogue signal from the CEM was gated by a $200 \mu\text{s}$ integration window that opened immediately after each laser flash and the output of the gated integrator was averaged by a filter having time constant 0.2 s. The rate of frequency stepping in 0.1 MHz increments could be set so that 3–10 laser shots occurred at each step. Repeated 5–40 MHz scans of the integrated signal versus frequency over the resonance could be overlaid as necessary to achieve satisfactory signal-to-noise ratio.

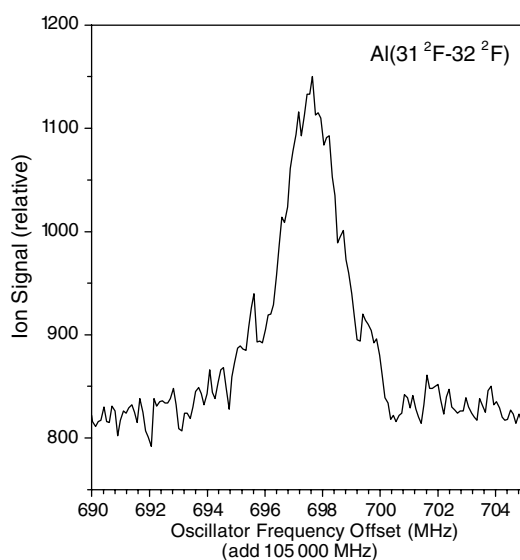


Figure 3. The measured line-shape of two-photon Al I $31\ ^2F-32\ ^2F$ microwave resonance. The summation of approximately 50 frequency scans for each transition is completed in about 10 min.

A typical result, the dependence of ion current upon frequency for the $31F \rightarrow 32F$ transition, is presented in figure 3. The line centre is determined graphically or by fitting to a symmetrical line-shape function. The main line-centre uncertainties were caused by shifts and asymmetrical broadening in inhomogeneous static electric fields and by ac Stark shifts caused by the relatively strong microwave fields necessary to drive the two-photon transitions. With care we were able to control the static stray-field effects, reconditioning the SFI plates to remove condensed Al coatings as necessary. Test measurements were performed on the $30F \rightarrow 31F$ resonance with (alternately) 60 and 0 mV bias applied across the ionization plates, with the result that a centre frequency shift 1.0 ± 0.1 MHz of the resonance was recorded. A shift of approximately the same size was noted between a condition of freshly cleaned plates and plates contaminated by deposits of Al and Al_2O_3 after several evacuation and depressurization cycles. On the basis of this observation, resonances were considered acceptable only when measured immediately after plate cleaning and re-evacuation. The ambient magnetic field was not cancelled, but its effect, if any, on the line-shapes is expected to be symmetrical. The applied microwave power was reduced until narrow and symmetrical resonance contours were achieved. In addition the laboratory operates in an environment of powerful radio-frequency and microwave backgrounds from nearby transmitters, sometimes preventing or delaying successful measurement. Because line-shifts doubtless remain from uncontrolled perturbations, we believe an energy splitting uncertainty of ± 1 MHz is appropriate for these results.

3. Results and discussion

The frequencies $\Delta\nu_{n,n+1}$ of nine two-photon transitions in the Rydberg series $n\ ^2F \rightarrow (n+1)\ ^2F$ were measured and assigned (see table 1). The standard-deviation uncertainties of oscillator frequencies in these measurements do not exceed 0.5 MHz (2×10^{-5} cm $^{-1}$). The energy separations are given by $2hc\Delta\nu_{n,n+1}$, where h is Planck's constant and c is the speed of light.

Table 1. Observed resonance line centres of Al I two-photon $nF \rightarrow (n+1)F$ transitions. (The energy level separations correspond to *twice* the oscillator frequencies given here.) The separations fit a model of the form given in equations (1) and (2) with a root mean square deviation less than $h \times 0.3$ MHz.

Transition	Centre frequency (MHz)
29 $^2F \rightarrow 30$ 2F	128 727.58
30 $^2F \rightarrow 31$ 2F	116 457.19
31 $^2F \rightarrow 32$ 2F	105 697.61
32 $^2F \rightarrow 33$ 2F	96 224.30
33 $^2F \rightarrow 34$ 2F	87 850.05
34 $^2F \rightarrow 35$ 2F	80 420.67
35 $^2F \rightarrow 36$ 2F	73 805.26
36 $^2F \rightarrow 37$ 2F	67 896.08
37 $^2F \rightarrow 38$ 2F	62 601.16

Table 2. Quantum-defect Ritz-expansion coefficients for Al I $3s^2nf$ 2F terms as derived from fits of present and earlier data to equations (1) and (2). Standard deviations are given in parentheses in terms of the last digit shown.

Transition data set	E_F	A_F	B_F
Present work	0.039 16(8)	-0.11(4)	—
Reference [4]	0.039 2649	-0.166 365	0.071 74
Reference [7]	0.038 94	-0.154	—
Present work + [4] and [7] (adjusted)	0.039 236(11)	-0.165 7(5)	0.068(6)

The 2F_j -state ($\ell = 3$) energy levels of Al I, corresponding to principal quantum number n , orbital angular momentum ℓ and total electronic angular momentum j , may be expressed by the Rydberg formula

$$E(n, \ell, j) = -\frac{hcR_{Al}}{n^{*2}} = -\frac{hcR_{Al}}{(n - \delta_{n,\ell,j})^2}. \quad (1)$$

The Ritz expansion of the quantum defect δ [13] may be written as

$$\delta_{n,\ell,j} = E_{\ell,j} + \frac{A_{\ell,j}}{n^{*2}} + \frac{B_{\ell,j}}{n^{*4}}. \quad (2)$$

Constants $E_{\ell,j}$ and $A_{\ell,j}$ (table 2) were obtained by least-squares fitting of data from table 1. The reduced-mass-corrected Rydberg constant for Al R_{Al} was taken to be $109\,735.08\text{ cm}^{-1}$ and the ionization limit was $48\,278.37\text{ cm}^{-1}$ [10]. (In previous work, as well as the present work, no F-state doublet splittings in this Rydberg series have ever been resolved—calculated hydrogenic values for $n = 4$ and 5 were introduced by Eriksson and Isberg [4]—so reference to the quantum number j will be omitted in the following.) The data were fitted in several ways to account for previous optical measurements [4, 7]. In the first line of the table are the fitted constants E and A based on the present measurements only. One-standard-deviation uncertainties of the coefficients are indicated by parentheses in terms the last digit given. The data of Eriksson and Isberg [4] correspond to Al I wavelength measurements of $3^2D_{3/2,5/2} \rightarrow n^2F_{5/2,7/2}$ transitions for $n = 4$ – 8 , from which those authors obtained values E , A and B given in the second line of the table. (The authors quoted no uncertainties in these coefficients.) The data of Zherikhin *et al* [7] correspond to measurements of the same optical transition series for $n = 11$ – 55 and the authors obtained from them the values E and A given in the third line.

The three sets of quantum-defect coefficients are not entirely consistent. By using the wavenumbers of $3^2P_{1/2} \rightarrow 3^2D_{3/2}$ and $3^2P_{3/2} \rightarrow 3^2D_{5/2}$ transitions implied by the NIST

database [10] (32 435.453 and 32 324.735 cm^{-1} , respectively), we have found that the results of the present work can be combined consistently with those of [4]. On the other hand, any joint fit of the results of [7] with the other two data sets reveals a systematic unidirectional deviation of the Zherikhin *et al* values by approximately 0.08 cm^{-1} . The fits assumed measurement uncertainty ± 1 MHz for our frequency intervals and the stated uncertainties of the other works: for [4]: ± 0.01 cm^{-1} ; and for [7]: ± 0.05 cm^{-1} . Note that in order to reconstruct the level energies and splittings from the Ritz coefficients in table 2, an iterative procedure must be followed [13], since the quantum defect δ appears implicitly on the right-hand side of equation (2). Convergence is very rapid. Once $\delta_{n,\ell}$ is determined for a given n , that value may be substituted directly into equation (1) to find the term energy.

We believe that the observed frequencies of [7] are systematically high—corresponding to F-state quantum defects that are slightly too small—due perhaps to systematic error in wavelengths in the neon hollow-cathode discharge that were selected as benchmarks in wavelength measurements of the $3^2\text{D}_{3/2,5/2} \rightarrow n^2\text{F}_{5/2,7/2}$ transitions. It is also likely that this caused an overestimate by 0.05 cm^{-1} of the ionization limit obtained in that work [7]. By reducing the frequencies from Zherikhin *et al* by a constant value 0.08 cm^{-1} and making a joint fit of these adjusted data together with our measurements and those of [4] we obtained good agreement for all observed frequencies. The resulting set of three quantum-defect coefficients E , A and B is given in the last line of table 2 and is the set that we believe best represents the true case. They differ only slightly from those of [4] but their uncertainties are explicitly given and their predictive value is confirmed by the present work for very high $n\text{F}$ terms.

On the basis of the hydrogenic 5^2F doublet splitting of 0.004 cm^{-1} [4] we expect the doublet fine-structure intervals in the $n = 29\text{--}38$ range, which scale as n^{-3} , to be smaller than about 0.5 MHz and to be well hidden in the present experiments. In order to reveal these splittings, tighter control of stray fields as well as longer microwave exposure times will be required. The F terms are well described by the Rydberg–Ritz expressions, equations (1) and (2), showing that there is no observable perturbation of F terms by the distributed $3s3p^2$ state [14], which strongly influences the $n^2\text{D}$ Rydberg series in Al.

The experimental work and analysis reported here, including clarification of discrepancies in previous optically based results [4, 7], form a solid foundation for our future intended work at a similar level of accuracy with other (S, P, D and G) angular momentum Rydberg states of Al I.

Acknowledgments

The research described in this publication was made possible in part by Award No UP1-2422-KH-02 of the US Civilian Research and Development Foundation for the Independent States of the Former Soviet Union (CRDF). The authors are grateful to M Efimenko and E Alekseev for their assistance in creation of the experimental set-up and to V Ilyushin for computer control programming.

References

- [1] Neijzen J H M and Dönszelmann A 1982 *Physica C* **114** 241
- Neijzen J H M and Dönszelmann A 1982 *Physica C* **114** 399
- Davidson M D, Buurman E P and Dönszelmann A 1990 *Z. Phys. D* **15** 293
- Hong F L, Maeda H, Matsuo Y and Takami M 1995 *Phys. Rev. A* **51** 1994
- Kasimov A K, Tursunov A T and Tukhlibaev O 1998 *Opt. Spectrosc.* **84** 482
- Alimov U Z, Muzhdabaev I S, Tukhlibaev O and Tursunov A T 2001 *Opt. Spectrosc.* **90** 808

- [2] Letokhov V S 1987 *Laser Photoionization Spectroscopy* (New York: Academic)
Hurst G S and Payne M G 1988 *Principles and Applications of Resonance Ionization Spectroscopy* (Philadelphia, PA: Hilger)
Zilliacus R and Likonen J 1992 *Appl. Spectrosc.* **46** 1828
- [3] Carvallo R M and Nagar N M 2000 *Astron. J.* **120** 1364
Daflon S, Cunha K, Smith V V and Butler K 2003 *Astron. Astrophys.* **399** 525
- [4] Eriksson K B S and Isberg H B S 1963 *Ark. Fys.* **23** 527
- [5] Eriksson K B S and Isberg H B S 1967 *Ark. Fys.* **33** 593
- [6] Buurman E P, Koning O J and Dönszelmann A 1989 *J. Phys. B: At. Mol. Opt. Phys.* **22** 3965
- [7] Zherikhin A N, Mishin V I and Fedoseev V N 1984 *Opt. Spectrosc.* **57** 476
- [8] Gallagher T F, Hill R M and Edelstein S A 1976 *Phys. Rev. A* **13** 1448
- [9] Gallagher T F 1994 *Rydberg Atoms* (New York: Cambridge University Press) pp 340–94
- [10] National Institute of Standards and Technology (NIST) 2003 *Atomic Spectra Database*
http://physics.nist.gov/cgi-bin/AtData/main_asd
- [11] O'Mahony P F 1985 *Phys. Rev. A* **32** 908
- [12] Strong J 1938 *Procedures in Experimental Physics* (New York: Prentice-Hall) pp 171–7
- [13] Drake G W F 1994 *Adv. At. Mol. Opt. Phys.* **32** 93
- [14] Theodosiou C E 1992 *Phys. Rev. A* **45** 7756